

## Accounting for Spin Relaxation in Quantitative Pulse Gradient Spin Echo NMR Mixture Analysis

Brian Antalek

Research and Development, Eastman Kodak Company, 1999 Lake Avenue, Rochester, New York 14650-2132

Received April 13, 2006; E-mail: brian.antalek@kodak.com

Characterizing mixtures is a complex process, especially when the components are chemically similar. Pulsed gradient spin echo (PGSE) NMR, coupled with various data processing schemes, has been used to perform mixture analysis.<sup>1–7</sup> Separation is based on differences in solution diffusivity (i.e., hydrodynamic size). Applications to polymer analysis,<sup>8–9</sup> protein binding,<sup>10</sup> and process monitoring<sup>11</sup> have recently been described. One drawback is that PGSE NMR is inherently nonquantitative. Because the experiment is echo-based, differences in the relaxation behavior of the nuclei among the components give rise to varied intensities and lead to nonquantitative spectra. This work describes a direct method to obtain resolved, quantitative spectra from mixtures.

Of the several data processing schemes available, one that is particularly useful for resolving mixture spectra having high spectral overlap is the direct exponential curve resolution algorithm (DECRA).<sup>4,12–14</sup> DECRA resolves pure component spectra and the respective diffusivities and has several advantages. It is computationally fast and, with only a small number of acquired spectra, can separate highly overlapped components, which have diffusion coefficients that differ by as little as 30%. The method presented here re-establishes quantitative information by combining the DECRA analysis of several PGSE NMR experiments obtained by using different delay times in the pulse sequence. From the results, quantitative spectra of the resolved components are extrapolated. The method is named quantitative DECRA (qDECRA).

Figure 1 illustrates the stimulated echo pulse sequence commonly used in PGSE NMR experiments. The solid boxes represent radio frequency,  $\pi/2$ , pulses, and the hatched boxes represent gradient pulses. The following equation describes the signal attenuation of the spectrum obtained from the Fourier transform of the half-echo<sup>3</sup>

$$E(q, \nu) = \sum_n A_n(\nu) \exp[-D_n q^2 (\Delta - \delta/3) - R] \quad (1)$$

where  $q = \gamma g \delta$ ,  $\gamma$  is the gyromagnetic ratio of the nucleus ( $\text{rad } T^{-1} \text{ s}^{-1}$ ),  $g$  is the gradient pulse strength ( $T \text{ m}^{-1}$ ),  $\delta$  is the gradient pulse width (s), and  $\Delta$  is the effective diffusion time.  $A_n(\nu)$  is the amplitude at a frequency value of the  $n$ th pure component in solution having a diffusion coefficient of  $D_n$ .  $R$  is equivalent to  $2\tau_1/T_2 + \tau_2/T_1$  and accounts for signal attenuation that is due to relaxation.  $T_1$  and  $T_2$  are exponential time constants that describe the longitudinal and transverse relaxation, respectively, of the nuclei within the sample. The greater the relaxation differs among the components or the different moieties within each component, the more the final spectral intensities deviate from the true values. For example, because of reduced molecular mobility, chemical species associated with solid surfaces will have shorter relaxation times than those that are unassociated and, therefore, will have spectra that experience relatively more signal loss.

An oleic acid/nanoparticulate zirconia dispersion in  $\text{CD}_2\text{Cl}_2$  (20 mg/mL, 5 nm  $\text{ZrO}_2$ ) is examined. Quantification of the oleic acid partitioning is desired. The carboxylic acid group of the oleic acid

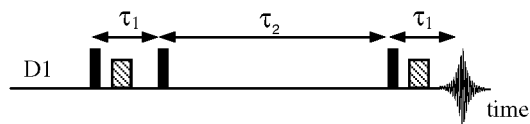


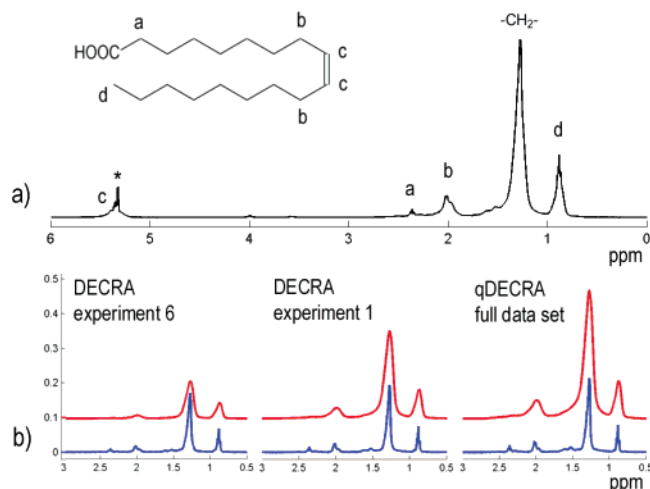
Figure 1. Stimulated echo pulse sequence.

forms a strong hydrogen bond to the surface of the metal oxide, and exchange is slow on the NMR time scale.<sup>15</sup> Because the diffusivity of the adsorbed oleic acid is much lower than the free oleic acid, PGSE NMR is well suited to address the problem. Because of reduced molecular mobility, relaxation times of the bound oleic acid are shorter, and the spectrum is broader than that of the free material.

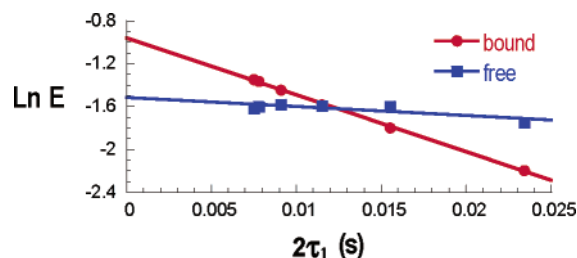
Experiments were performed on a Varian Inova NMR spectrometer, operating at a  $^1\text{H}$  frequency of 400 MHz using a standard 5 mm,  $z$ -gradient probe. A stimulated echo pulse sequence employing two bipolar gradient-pulse composites was used.<sup>16</sup> Six PGSE NMR experiments were performed with varied  $\tau_1$  and  $\tau_2$  delays.  $\tau_1$  and  $\tau_2$  are varied simultaneously but have the same ratio,  $\alpha = \tau_1/\tau_2$ , in each experiment. This is key in enabling a simple linear least-squares analysis. The values used for  $2\tau_1$  are 0.00745, 0.00785, 0.00905, 0.01145, 0.01545, and 0.02345 s. The values used for  $\tau_2$  are 0.149, 0.157, 0.181, 0.229, 0.309, and 0.469 s. Ten spectra were collected in each experiment with the same varied gradient strength,  $g$ : 2.00, 30.06, 42.46, 51.98, 60.02, 67.10, 74.49, 79.38, 84.85, and 90.00  $\text{G cm}^{-1}$ . These are varied so that the difference in  $g^2$  is a constant, a necessary condition for DECRA analysis. A value of 10 s, which is longer than 5 times the longest  $T_1$  found in the sample, was chosen for D1. Temperature was controlled at 23 °C.

Figure 2a shows the  $^1\text{H}$  NMR spectrum of the zirconia dispersion. Evidence of the narrower spectrum of the free oleic acid is seen in superposition to the broader spectrum of the bound oleic acid. The DECRA analyses of the sixth and first experiments are shown in Figure 2b. Three components are resolved: bound oleic acid (red; top); free oleic acid (blue; bottom); and solvent (not shown). The mole percent bound oleic acid, calculated from the integral areas, is 56 and 74% for the sixth and first experiments, respectively. The differences in relaxation rates between the bound and free populations are evident in comparing the results of the two experiments. The difference in signal between the bound and free is greater for experiment 6 compared to experiment 1. Therefore, the true fraction of bound material is underestimated. Furthermore, the difference in relaxation between the methylene groups and the methyl group within the resolved bound component is seen when comparing experiments 6 and 1.

The procedure used to arrive at the correct value for the bound fraction is straightforward. The DECRA analysis is performed on each experiment and provides the  $g = 0$  spectra. A series of six spectra for each DECRA-resolved component are used to extrapolate the quantitative spectrum for each component. This is done point-by-point above a noise threshold in the spectra. Figure 3 shows



**Figure 2.** (a)  $^1\text{H}$  NMR spectrum of the zirconia dispersion in  $\text{CD}_2\text{Cl}_2$ . (b) From left to right, DECRA results of the sixth experiment and the first experiment and qDECRA results of the full data set.



**Figure 3.** Semilog plot of signal at the peak of the methylene resonance (1.2 ppm) within the resolved spectra of bound and free oleic acid as a function of the delay time,  $\tau_1$ .

a semilog plot of the signal at the peak of the methylene resonance (1.2 ppm) within the six resolved spectra of both bound and free oleic acid. As the delay times approach zero, the signal approaches the quantitative value. The fact that the data is collected with a constant ratio  $\alpha$  greatly simplifies the analysis.  $R$  in eq 1 can be expressed as a constant multiplied by  $\tau_1$  (or  $\tau_2$ ). Plotting  $\ln E$  versus  $\tau_1$  is exactly the same as plotting  $\ln E$  versus  $\tau_2$  with only a scaling factor in the  $x$  variable (i.e., only the slope differs). Therefore, only one linear equation is necessary for extrapolation to the delay = 0 value.

$$\ln E = a + b\tau_1 \quad (2)$$

$a$  is the  $y$  intercept (i.e., the quantitative point), and slope  $b = -(2/T_2 + 1/\alpha T_1)$ . From eq 2, the normal equations are constructed<sup>17</sup>

$$an + b\sum\tau_1 = \sum\ln E; \quad a\sum\tau_1 + b\sum\tau_1^2 = \sum\tau_1 \ln E \quad (3)$$

where  $n$  is the number of experiments, six. The set of linear equations (3) is then solved directly for the variable,  $a$ , using MATLAB (The Mathworks, Inc., Natick, MA; version 6.1; Windows 2000). The procedure is performed for each frequency point in the three resolved spectral series (bound, free, and solvent) to produce the three quantitative spectra.

Figure 2b shows the qDECRA result. All three results shown in Figure 2b are plotted in absolute mode and can be compared directly with one another. While the free oleic acid component is nearly identical in all three analyses, the intensity for the bound species differs significantly. The corrected mole-percent bound oleic acid derived from qDECRA in Figure 2b is 80%. This was verified using

spectral deconvolution on a portion of the normal NMR spectrum, which produced a value of 82%.

The average diffusion coefficients of the three resolved components are  $40.6 \pm 3.5$ ,  $9.54 \pm 0.76$ , and  $1.51 \pm 0.02 \times 10^{-10} \text{ m}^2 \text{ s}^{-1}$  for the solvent, free oleic acid, and bound oleic acid, respectively. The hydrodynamic diameter of the zirconia–oleic acid composite estimated from the bound oleic acid diffusion coefficient using the Stokes–Einstein relationship is 6.8 nm.<sup>18</sup> This is close to what is expected for the 5 nm  $\text{ZnO}_2$  particles with monolayer coverage. Because both DECRA and the subsequent quantitative analysis are direct (i.e., no iterative procedure), the total processing time is extremely short. For the data set presented here, including 60 spectra with 13 000 real data points each, the processing time is about 10 s with a mid-level PC.

qDECRA is well-suited for the analysis of adsorbed species because of the high spectral overlap and large differences in relaxation between the two populations. For example, the study of composites used for biomedical probes,<sup>19</sup> where the technology depends on adsorption of various species on a nanosized substrate, would particularly benefit from qDECRA. Another area of potential benefit is the analysis of polymeric solutions, where there tends to be a large range in relaxation values. For example, flexible segments such as those containing ethylene glycol groups tend to have long relaxation times, and stiffer segments, such as vinyl backbones, have much shorter relaxation times.

There are limitations to this approach. Low signal-to-noise and gradient field nonuniformity will limit the ability to resolve spectra. Effects of chemical exchange, cross-relaxation, and  $J$ -modulation (from strong homonuclear coupling) lead to nonquantitative conditions.

**Acknowledgment.** The author thanks Jin-Shan Wang and Kevin Dockery for providing the dispersion, as well as J. Michael Hewitt and Willem Windig for their valuable discussions.

**Supporting Information Available:** MATLAB scripts of qDECRA and DECRA. This material is available free of charge via the Internet at <http://pubs.acs.org>.

## References

- (1) Stejskal, E. O.; Tanner, J. E. *J. Chem. Phys.* **1965**, *42*, 288–292.
- (2) Stilbs, P. *Prog. Nucl. Magn. Reson. Spectrosc.* **1987**, *19*, 1–45.
- (3) Johnson, C. S., Jr. *Prog. Nucl. Magn. Reson. Spectrosc.* **1999**, *34*, 203–256.
- (4) Antalek, B. *Concepts Magn. Reson.* **2002**, *14*, 225–258.
- (5) Huo, R.; Geurts, C.; Brandis, J.; Wehrens, R.; Buydens, L. M. C. *Magn. Reson. Chem.* **2006**, *44*, 110–117.
- (6) Stilbs, P.; Paulsen, K.; Griffiths, P. C. *J. Phys. Chem.* **1996**, *100*, 8180–8189.
- (7) Morris, G. A. *Encyclopedia of Nuclear Magnetic Resonance*; Wiley & Sons: New York, 2002; Chapter 9, pp 35–44.
- (8) Jerschow, A.; Mueller, N. *Macromolecules* **1998**, *31*, 6573–6578.
- (9) Antalek, B.; Hewitt, J. M.; Windig, W.; Yacobucci, P. D.; Mourey, T.; Le, K. *Magn. Reson. Chem.* **2002**, *40*, S60–S71.
- (10) Lucas, L. H.; Larive, C. K. *Concepts Magn. Reson.* **2004**, *20*, 24–41.
- (11) Nordon, A.; Meunier, C.; Carr, R. H.; Gemperline, P. J.; Littlejohn, D. *Anal. Chim. Acta* **2002**, *472*, 133–140.
- (12) Antalek, B.; Windig, W. *J. Am. Chem. Soc.* **1996**, *118*, 10331–10332.
- (13) Zumbulyadis, N.; Antalek, B.; Windig, W.; Scaringe, R. P.; Lanzafame, A. M.; Blanton, T.; Helber, M. *J. Am. Chem. Soc.* **1999**, *121*, 11554–11557.
- (14) Windig, W.; Antalek, B.; Sorriero, L.; Bijlsma, S.; Louwse, D. J.; Smilde, A. *J. Chemom.* **1999**, *13*, 95–110.
- (15) Pawsey, S.; Yach, K.; Halla, J.; Reven, L. *Langmuir* **2000**, *16*, 3294–3303.
- (16) Wu, D.; Johnson, C. S. *J. Magn. Reson., Ser. A* **1995**, *115*, 260.
- (17) Bates, D. M.; Watts, D. G. *Nonlinear regression analysis and its applications*; Wiley: New York, 1988.
- (18)  $D = kT/6\pi\eta R_H$ , where  $k$  ( $\text{J K}^{-1}$ ) is the Boltzmann constant,  $T$  is the temperature (K),  $\eta$  (0.000421 P) is the solvent viscosity, and  $R_H$  (m) is the hydrodynamic radius.
- (19) Choy, G.; Choyke, P.; Libutti, S. K. *Mol. Imaging* **2003**, *2*, 303–312.

JA062592C